Neuroscience Research 215 (2025) 56–63

Contents lists available at ScienceDirect

Neuroscience Research

journal homepage: www.sciencedirect.com/journal/neuroscience-research

Review article

Probing neuronal activity with genetically encoded calcium and voltage fluorescent indicators

Masayuki Sakamoto *, Tatsushi Yokoyama

Graduate School of Biostudies, Kyoto University, 53 Shogoin Kawara-cho, Sakyo-ku, Kyoto 606-8507, Japan

ARTICLE INFO

Keywords:
Calcium imaging
Voltage imaging
In vivo imaging
Fluorescent protein
Protein engineering

ABSTRACT

Monitoring neural activity in individual neurons is crucial for understanding neural circuits and brain functions. The emergence of optical imaging technologies has dramatically transformed the field of neuroscience, enabling detailed observation of large-scale neuronal populations with both cellular and subcellular resolution. This transformation will be further accelerated by the integration of these imaging technologies and advanced big data analysis. Genetically encoded fluorescent indicators to detect neural activity with high signal-to-noise ratios are pivotal in this advancement. In recent years, these indicators have undergone significant developments, greatly enhancing the understanding of neural dynamics and networks. This review highlights the recent progress in genetically encoded calcium and voltage indicators and discusses the future direction of imaging techniques with big data analysis that deepens our understanding of the complexities of the brain.

1. Introduction

The brain is composed of an extensive and intricate network of neurons, ranging in number from hundreds of millions to billions. These neurons connect in complex patterns and form circuits that process and interpret large amounts of information, playing a crucial role for the execution of higher brain functions, such as cognition and learning. Therefore, probing functional neural circuits at a high spatiotemporal resolution is crucial for understanding how neuronal populations work together to generate internal brain states and behaviors. This research is pivotal not only for exploring the fundamental principles of the brain function but also for addressing neurological and psychiatric diseases. To address these questions, it is essential to simultaneously measure neural activity from numerous neurons (Yuste and Bargmann, 2017).

Electrophysiological approaches using electrodes, such as patch-clamp recording, have traditionally been the gold standard for measuring membrane potential (Neher and Sakmann, 1976). However, these electrode-based methods often lack spatial resolution and genetic specificity. Optical imaging with genetically encoded indicators can overcome these drawbacks, enabling the monitoring of large neuronal populations simultaneously with cellular or even subcellular resolution. In addition, recently, the rapid growth of big data analysis technologies has further revolutionized this field. The integration of optical imaging with advanced big data analysis marks a new era in neuroscience, unlocking complex and previously inaccessible insights (Landhuis, 2017). The application of machine learning algorithms and other advanced computational methods to imaging datasets has opened new avenues for understanding complex biological systems. These methodologies are crucial for advancing the understanding of various physiological and pathological conditions, including neural development and synaptic plasticity, and the mechanisms underlying neurodegenerative diseases, thereby providing unprecedented insights into brain function (Schneider et al., 2023). To effectively utilize imaging technologies, genetically encoded fluorescent indicators that can detect neural activity with a high signal-to-noise ratio are essential, as well as sophisticated analysis techniques. In recent years, the field of fluorescent probes has demonstrated remarkable growth and advancement, providing more comprehensive understanding of neural dynamics and networks in the brain.

In this review, we will introduce recent advancements in the design and application of genetically encoded calcium and voltage indicators. In addition, we will discuss future perspectives on the integration of imaging techniques with big data analysis that promises to deepen our understanding of the complexities of the brain.

2. Calcium imaging

Calcium ions (Ca^{2+}) play a crucial role in regulating a variety of

* Corresponding author.
E-mail address: sakamoto.masayuki.2e@kyoto-u.ac.jp (M. Sakamoto).

https://doi.org/10.1016/j.neures.2024.06.004
Received 6 February 2024; Received in revised form 9 April 2024; Accepted 8 June 2024
Available online 15 June 2024

cellular functions, including neural activity and muscle contraction. In cortical neurons, the concentration of intracellular free Ca^{2+} is maintained at a low level, typically ranging between 30 and 100 nM, when the neuron is in a resting state with a membrane potential of around −70 mV (Grienberger and Konnerth, 2012). When action potentials occur, Ca^{2+} influx into the neuron through voltage-gated calcium channels and other pathways. This influx leads to a temporary spike in calcium concentration within the soma, often increasing by 10–100-fold compared to the resting state, significantly impacting neuronal processes (Berridge et al., 2000). Simultaneous *in vivo* calcium imaging and electrophysiology in the same neuron have revealed a correlation between calcium signaling in the soma and neuronal firing (Wei et al., 2020). Given its pivotal role, calcium imaging has emerged as a popular method for measuring neuronal activity. It enables visualization and quantification of changes in calcium concentrations, providing valuable insights into how neurons behave and communicate. Calcium imaging has now become an indispensable technique in the field of neuroscience.

Various fluorescent probes have been developed to visualize calcium dynamics in living cells. A pioneering study in this field was conducted by Tsien and colleagues in the early 1980s. They developed the first calcium-sensitive fluorescent dye, Quin-2 (Tsien et al., 1982). Following this seminal development, a variety of highly sensitive dyes, such as Fura-2, Indo-1, and Fluo-4, were introduced (Gee et al., 2000; Grynkiewicz et al., 1985). While a revolutionary technique, the application of these dyes was limited by the need for delivery through glass pipettes or bulk extracellular loading, which constrained cell-type-specific targeting and imaging conditions. Genetically encoded calcium indicators (GECIs) have overcome these limitations, enabling long-term, repetitive, and unbiased functional imaging of specific types of neurons and even subcellular compartments.

3. FRET-type GECIs

The initial GECI developed by Miyawaki and colleagues was based on Förster resonance energy transfer (FRET) (Miyawaki et al., 1997). This FRET-type GECI can detect changes in Ca^{2+} concentrations by measuring the ratio of fluorescence intensity between two fluorescent proteins, cyan fluorescent protein (CFP) and yellow fluorescent protein (YFP), linked by peptides consisting of the calmodulin (CaM) and the calmodulin-binding peptide of myosin light chain kinase (M13) (Fig. 1A). In the absence of Ca^{2+}, the emission is primarily from CFP. In the presence of Ca^{2+}, intramolecular conformational changes alter the

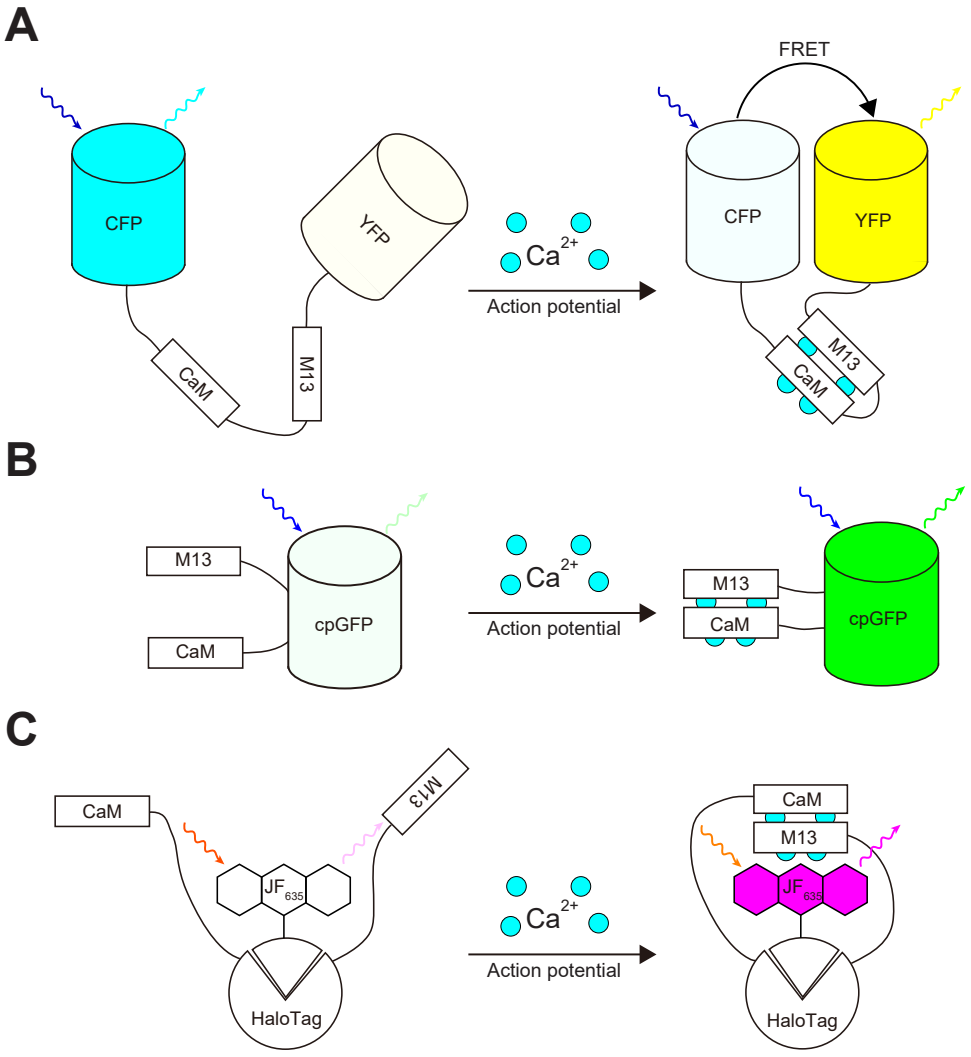

Fig. 1. Genetically encoded calcium indicators. (A) FRET-based GECI design. In the absence of Ca^{2+}, the emission is primarily from CFP. After binding Ca^{2+}, intramolecular conformational changes lead to a reduction of the spatial distance between CFP (donor) and YFP (acceptor). This enables Förster resonance energy transfer (FRET), resulting in a decrease in CFP fluorescence and an increase in YFP fluorescence. (B) Single-fluorophore GECI design. The Ca^{2+} binding induces conformational intramolecular changes, leading to an increase in the emitted fluorescence. (C) Chemigenetic GECIs design. HaloTag domain is used to bind fluorescent synthetic dyes. After binding Ca^{2+}, conformational changes result in an increase in the emitted fluorescence.

spatial distance between CFP and YFP, resulting in decreased CFP fluorescence and increased YFP fluorescence. Thus, changes in the CFP and YFP emission spectrum correlate with variations in intracellular Ca^{2+} concentration, enabling ratiometric imaging through quantification of the YFP/CFP ratio. Subsequently, more sensitive sensors were developed with other fluorescent proteins and calcium-binding proteins (Nagai et al., 2004; Thestrup et al., 2014). One of the advantages of ratiometric imaging is its ability to reduce noise, such as motion artifacts (Michikawa et al., 2021). However, later generations of GECIs have predominantly utilized a single-fluorophore design.

4. Single-fluorophore GECIs

The most frequently used intensiometric fluorescent GECI was G-CaMP, developed by Nakai and colleagues (Nakai et al., 2001). G-CaMP consists of a circularly permuted green fluorescent protein (cpGFP), CaM, and M13 peptide (Fig. 1B). When Ca^{2+} binds to G-CaMP, it causes a conformational change, resulting in increased fluorescence intensity. However, earlier versions of intensiometric fluorescent GECIs lacked sufficient sensitivity, rendering them unsuitable for *in vivo* imaging. The development of GCaMP6 and its successor jGCaMP7 series from the Janelia Research Campus marked significant improvements, making GECIs widely applicable for measuring neural activity both *in vitro* and *in vivo* (Table 1) (Chen et al., 2013; Dana et al., 2019). While previous GECIs were not as effective as Ca^{2+}-sensitive organic dyes like Oregon Green BAPTA-1 (OGB-1), the GCaMP6 series demonstrated superior performance in detecting action potentials. Notably, the GCaMP6 series could detect electrical activity in neuropils such as dendritic spines with high signal-to-noise ratio. Additionally, genetic approaches like Cre/-loxP system further enabled cell-type-specific imaging. GECIs can also be stably expressed in cells over extended periods, facilitating long-term imaging which was not achieved by calcium-sensitive dyes. These advancements facilitated monitoring neural activity during the learning process not only in rodents but also in non-human primates (Chu et al., 2016; Ebina et al., 2018). Beyond two-photon microscopy, fiber photometry and microendoscopy have become viable methods for calcium imaging in freely moving animals (Karigo et al., 2021; Kondo et al., 2018; Yukinaga et al., 2022). Despite the widespread adoption of GECIs, they still have limitations in their temporal resolution, affecting their ability to precisely decode the timing and number of spikes in individual neurons. Recent developments of GECIs have aimed to improve the accuracy and reliability of capturing neural activity.

To address this issue, Bito and colleagues redesigned the original GCaMPs by substituting the M13 with a different Ca^{2+}/CaM-binding peptide from Ca^{2+}/CaM-dependent protein kinase kinase (CaMKK) (Inoue et al., 2015). This modification led to the generation of a new calcium sensor, XCaMP, which exhibits greater sensitivity and linearity in response to Ca^{2+} concentration changes compared to existing sensors (Inoue et al., 2019). XCaMP-Gf represented a significant improvement over GCaMP6, featuring a 2.5-fold increase in signal-to-noise ratio for detecting single action potentials, a 10-fold faster rise time, and decay time constants that are twice as fast. These features significantly improve its ability to accurately decode spike numbers and spike timings, especially in high-frequency firing parvalbumin-positive interneurons. Following a similar approach to XCaMP, the Janelia Research Campus introduced jGCaMP8, another fast and sensitive calcium sensor. In jGCaMP8, the M13 is replaced by a peptide derived from endothelial nitric oxide synthase (Table 1) (Zhang et al., 2023). These advanced sensors, with their improved sensitivity and kinetics, provide more precise detection of spike timings and frequencies compared to conventional GECIs.

Table 1
Comparative performance of GECIs.

GECI	ΔF/F (%)	Rise time, $t_{1/2}$ (ms)	Decay time, $t_{1/2}$ (ms)	K_d (nM)	Hill coefficient	Reference
Green[a]						
XCaMP-Gf	25	15.6	194	154	1.99	Inoue et al., (2019)
jGCaMP7f	23	26.8	297	150	3.10	Dana et al., (2019)
jGCaMP8f	37	6.6	87.5	334	2.08	Zhang et al., (2023)
Red[b]						
jRGECO1a	9	25.5	177	102	1.94	Dana et al., (2016)
XCaMP-R	~20	-	~195	97	1.1	Inoue et al., (2019)
RCaMP3	34	25.1	145	101	2.06	Yokoyama et al., (2024)

[a] : ΔF/F and kinetics in response to single action potentials were measured in cultured neurons. The dissociation constant (K_d) and Hill coefficient were determined from purified proteins.

[b] : ΔF/F and kinetics in response to single action potentials were measured in living mice. K_d and Hill coefficient were determined from HEK293T cell lysate (jRFECO1a and RCaMP3) and purified protein (XCaMP-R).

5. A color palette of GECIs

Conventionally, GECIs have primarily utilized GFP. Recent advancements in fluorescent proteins have expanded the color palette of GECIs. In particular, red GECIs, potentially similar capability to GCaMP with additional advantages, have become increasingly salient (Dana et al., 2019; Fenno et al., 2020; Inoue et al., 2015, 2019; Ohkura et al., 2012; Yokoyama et al., 2024; Zhao et al., 2011). In recent years, highly sensitive red GECIs have been applied for *in vivo* imaging (Table 1). One of the most significant applications of red GECIs is for multicolor imaging, which enables the simultaneous labeling and monitoring of different neuronal populations in distinct colors. For instance, using red and green calcium sensors into excitatory and inhibitory neurons, respectively, enables distinct visualization of their activities with cellular resolution (Dana et al., 2016; Inoue et al., 2015; Sakamoto et al., 2022). This approach extends beyond merely monitoring neuronal activity; it also facilitates the visualization of neuromodulators such as dopamine, serotonin, orexin, and oxytocin, as well as intracellular signaling molecules (Duffet et al., 2022; Ino et al., 2022; Unger et al., 2020; Yokoyama et al., 2024; Zhuo et al., 2023). Such broad applications provide deeper insights into the mechanisms of brain functions. Furthermore, due to the lower light scattering at longer wavelengths, red GECIs are suitable for deep brain imaging in areas such as hippocampal CA1 region and medial prefrontal cortex of the mouse brain (Inoue et al., 2019; Kondo et al., 2017). Red GECIs can also be effective for measuring neural activity in non-human primates with larger brains, such as common marmosets. In addition to red GECIs, recent developments have introduced a wider range of colors: blue (XCaMP-B) (Inoue et al., 2019), yellow (XCaMP-Y, jYCaMP, NEMO) (Inoue et al., 2019; Li et al., 2023; Mohr et al., 2020), and even near-infrared (NIR-GECO, iBB-GECO) (Hashizume et al., 2022; Qian et al., 2019). These indicators significantly enhanced the versatility of imaging tools in the field of neuroscience.

To achieve functional deep brain imaging, further development is necessary, particularly in enhancing chromophore properties such as brightness. Recent progress in this field is the development of a novel 'chemigenetic' fluorescent calcium indicator platform. This platform utilizes the self-labeling HaloTag protein, which is conjugated to synthetic fluorophores such as Janelia Fluor dye (Fig. 1C) (Deo et al., 2021). This approach yields brighter red and far-red GECIs suitable for deep brain imaging.

6. Voltage imaging

Although calcium imaging is a robust method for tracking neural

activity, the calcium dynamics revealed by GECIs are not a direct proxy of membrane potential changes. Thus, calcium imaging is limited in its ability to provide a complete description of neuronal activity. First, somatic calcium imaging captures predominantly action potentials (Smetters et al., 1999). Subthreshold excitatory or inhibitory synaptic inputs are practically invisible. Second, due to biophysical limitations, calcium dynamics are significantly slower than the timescale of membrane potential changes. This discrepancy makes it challenging to precisely determine the number of spikes and spike timing with calcium imaging when neurons fire a burst of spikes. Third, calcium dynamics are shaped by complicated interactions between ionic diffusion and extrusion, and they can be significantly altered by intrinsic and extrinsic calcium buffers and the expression of calcium indicators themselves (Neher, 1998). Given these constraints, calcium imaging with GECIs is not an ideal technique for capturing the entire spectrum of neural activity.

Voltage imaging can directly monitor the electrical activity of neurons, including subthreshold events, providing a more precise measurement of neuronal dynamics (Peterka et al., 2011; Storace et al., 2016; Zhang et al., 2021). In parallel with GECIs, substantial progress has been made in developing genetically encoded voltage indicators (GEVIs) since the initial GEVI, named Flash, was reported by Isacoff and colleagues (Siegel and Isacoff, 1997). These GEVIs can specifically target and measure neural activity in distinct types or subcellular compartments (Kwon et al., 2017). In addition, these indicators are capable of detecting subthreshold activity that is not detectable by calcium imaging, thereby enabling more accurate decoding of brain functions (Bando et al., 2019, 2021; Cornejo et al., 2022). Therefore, voltage imaging with GEVIs is becoming a potent alternative to calcium imaging. Recent advancements in GEVIs can primarily fall into two categories: 1) those utilizing voltage-sensitive domain (VSD) of voltage-sensitive phosphatase and 2) those utilizing microbial rhodopsins.

7. VSD-based GEVIs

Initially developed GEVIs were structured by fusing fluorescent proteins to voltage-sensitive ion channels. However, these early GEVIs were not practically usable as voltage sensors due to their poor membrane localization in mammalian cells and low signal-to-noise ratio. Since the discovery of a voltage-dependent phosphatase from *Ciona intestinalis* (Ci-VSP) in 2005, this has been utilized as the fundamental structure of GEVIs (Murata et al., 2005). The VSP comprises voltage-sensitive domains composed of four transmembrane helices (S1-S4). The S4 helix contains several positively charged amino acids, including arginine and lysine, which move in response to membrane potential changes (Akemann et al., 2010; Jin et al., 2012; Tsutsui et al., 2008). The VSD-based GEVIs incorporate a fluorescent protein adjacent to the S4 helix and detect membrane potential changes by monitoring fluorescence changes, which correlate with conformational changes. In recent years, highly sensitive VSD-based GEVIs employing *Gallus gallus (*Gg*)*-VSD have been developed. These are suitable for both one- or two-photon imaging, facilitating the measurement of membrane potential changes *in vivo* with single-cell resolution (Fig. 2A, Table 2) (Evans et al., 2023; Liu et al., 2022; Lu et al., 2023; Platisa et al., 2023; Villette et al., 2019).

8. Rhodopsin-based GEVIs

Microbial rhodopsins, consisting of rhodopsin apoprotein and light-absorbing chromophore retinal, serve as light-sensitive ion pumps, ion channels, and sensors (Zhang et al., 2021). These rhodopsins were initially utilized for optogenetic actuators (Boyden et al., 2005; Chow et al., 2010). However, due to the low quantum yield of the retinal chromophore, its fluorescence was overlooked in earlier studies. Cohen and colleagues found that Archaerhodopsin-3 (Arch), derived from *Halorubrum sodomense*, exhibits voltage-dependent fluorescent changes from the retinal chromophore in neurons, allowing to accurately monitor membrane potentials with high temporal resolution (Kralj et al., 2011). For voltage imaging, Arch and its variants are typically excited with red light (640 nm) and emit in the infrared spectrum (peak at around 715 nm) (Fig. 2B) (Kralj et al., 2011). The voltage sensitivity of these proteins is attributed to the protonation of the Schiff base in the photointermediate state (Maclaurin et al., 2013). However, their practical applications were initially limited due to weak fluorescence and an insufficient signal-to-noise ratio (Kojima et al., 2020). To address these problems, significant efforts, including mutagenesis related to the photocycle or near the Schiff base, have been made (Piatkevich et al., 2018). These efforts led to improved brightness and dynamic range. As a result, several GEVIs suitable for *in vivo* one-photon imaging have been developed, further advancing the field (Table 3) (Piatkevich et al., 2019; Tian et al., 2023).

9. eFRET-based GEVIs

Despite extensive efforts to Arch variants, their brightness remains lower than that of commonly used fluorescent proteins. To overcome this issue, an electrochromic Förster resonance energy transfer (eFRET) strategy was developed. Microbial rhodopsins have an absorption spectrum that overlaps with the emission spectrum of popular fluorescent proteins. Therefore, these fluorescent proteins and other chemical fluorophores can serve as FRET donors, while rhodopsin molecules can serve as FRET acceptors (Bayraktar et al., 2012). eFRET sensors detect the absorption change of rhodopsin through the quenching of an attached fluorescent protein's intensity. When neurons depolarize, the fluorescent protein intensity is decreased by FRET from the fluorescent protein to the rhodopsin (Fig. 2C) (Gong et al., 2014; Zou et al., 2014). Thus, FRET-opsin-based GEVIs detect voltage depolarization by the decrease in emission intensity from the fluorescence donor. The rhodopsins used in these GEVIs are not limited to Arch alone (Zou et al., 2014). Others like Mac (bacteriorhodopsin from *Leptosphaeria maculans*) and Ace2 (bacteriorhodopsin from *Acetabularia acetabulum*) were also successfully employed to generate new indicators with fast kinetics and high dynamic range (Gong et al., 2015, 2014; Kannan et al., 2022). Given the broad absorption spectrum of microbial rhodopsin, a variety of fluorescent proteins with different emission wavelengths can serve as donors, broadening the versatility of these GEVIs, enabling *in vivo* one-photon voltage imaging with single-cell resolution (Table 3) (Abdelfattah et al., 2019, 2020, 2023; Han et al., 2023; Kannan et al., 2022, 2018; Kojima et al., 2020). In addition, by utilizing optical fibers, these sensors can accurately detect oscillatory waves in the brain (Kannan et al., 2018; Marshall et al., 2016). Synthetic fluorescent dyes are also available as eFRET donors (Fig. 2D). Voltron includes a HaloTag domain that enables the use of Janelia Fluor dyes as the eFRET donor. These synthetic dyes are more photostable and brighter than the fluorescent proteins, facilitating *in vivo* one-photon voltage imaging. It is important to note, however, that both rhodopsin- and eFRET-based GEVIs tend to reduce voltage sensitivity under two-photon excitation (Bando et al., 2019; Maclaurin et al., 2013).

10. Discussion

Here, we introduced the recent progress of genetically encoded biosensors for monitoring neural activity by optical imaging. The development of GECIs and GEVIs helped significantly advance when decoding neural activity with high spatiotemporal resolution precisely. This development has opened new avenues in neuroscience research, particularly in visualizing activity in a subcellular domain, which was previously challenging with conventional electrophysiology (Chen et al., 2013; Cornejo et al., 2022; Kwon et al., 2017). The development of even more sensitive probes in the future is expected to elucidate circuit mechanisms of higher brain functions and biological phenomena that have not been elucidated.

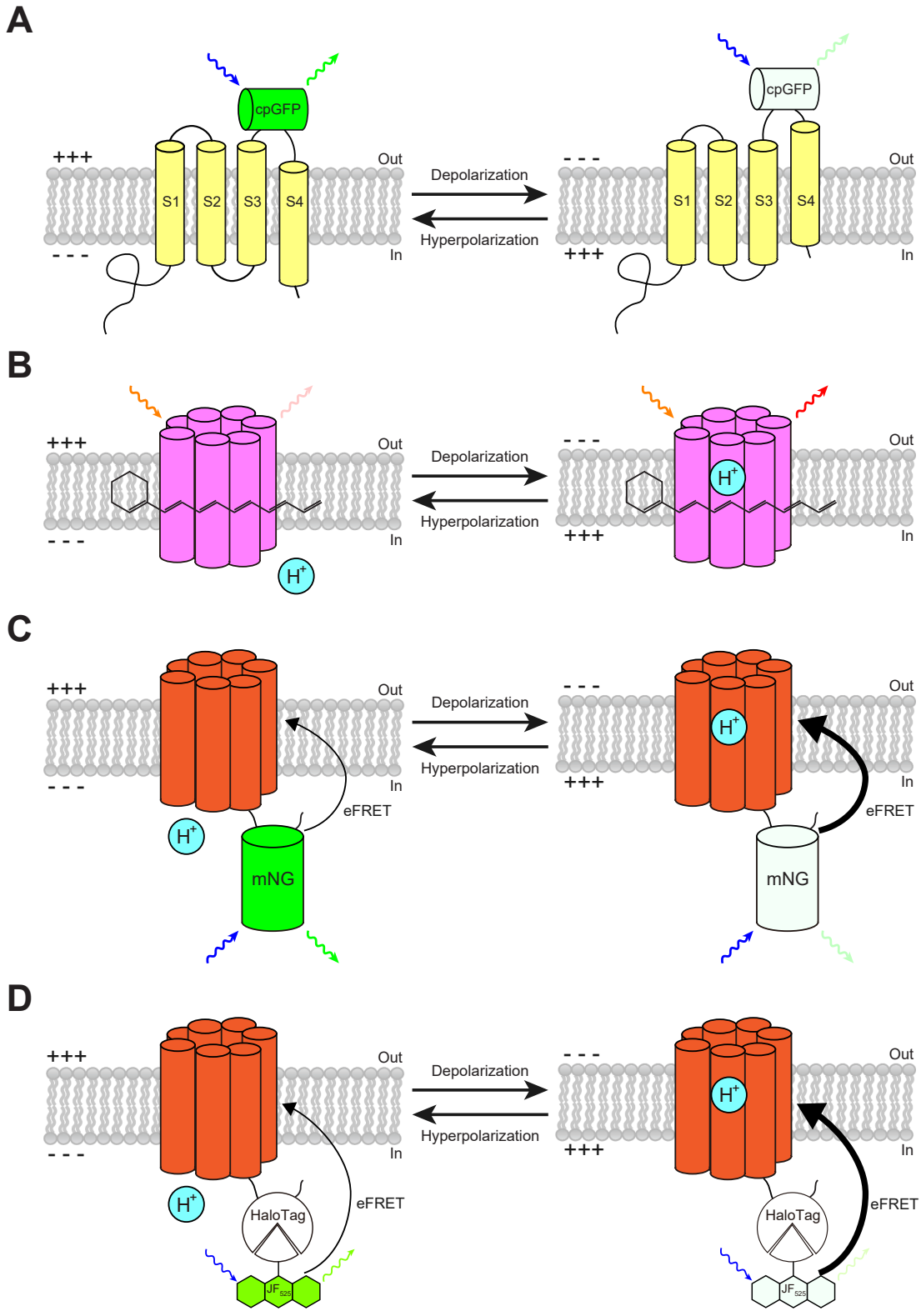

Fig. 2. Genetically encoded voltage indicators. (A) Voltage-sensitive domain (VSD)-based GEVIs. Voltage-dependent movement of a transmembrane S4 helix perturbs the protonation state of a fluorescent protein (cpGFP), resulting in changes in fluorescence emission. (B) Voltage sensing mechanism of microbial rhodopsin-based GEVIs. This type of sensor reports voltage changes through the fluorescence intensity changes of the retinal chromophore caused by protonation of the Schiff base in the photointermediate state. (C) Voltage sensing mechanism of microbial eFRET-based GEVIs (Ace2N-mNeon). At a depolarized stage, the Schiff base of microbial rhodopsin is protonated, and the absorbance of rhodopsin changes. This absorption quenches the fluorescence of the appended fluorescent proteins. (D) Chemigenetic GEVIs. The HaloTag domain is used to bind fluorescent synthetic dyes. Upon the depolarization, the Schiff base of microbial rhodopsin is protonated, leading to a change in the rhodopsin's absorbance. This absorption quenches the fluorescence of the appended bright fluorophores.

Table 2
Comparative performance of VSD-based GEVIs.

GEVI	Fluorophore	ΔF/F (%)	τ_{on} τ_1:τ_{on} fast (ms) τ_2:τ_{on} slow (ms) $\%_{\tau1}$: τ_1 component amplitude (%)			τ_{off} τ_1:τ_{off} fast (ms) τ_2:τ_{off} slow (ms) $\%_{\tau1}$: τ_1 component amplitude (%)			Reference
			τ_1 (ms)	τ_2 (ms)	$\%\tau_1$	τ_1 (ms)	τ_2 (ms)	$\%\tau_1$	
ASAP3	cpsfGFP	-51	2.6	26	76	23	93	84	Villette et al., (2019)
ASAP4e	cpsfGFP	210	3.9	21	14	8.4	18	21	Evans et al., (2023)
JEDI-1 P	cpsfGFP	-55	1.7	28	86	2.9[a]	-	-	Lu et al., (2023)
JEDI-2 P	cpsfGFP	-49	1.2	12	88	2.5[a]	-	-	Liu et al. (2022)
SpikeyGi2	cpsfGFP	58	-	-	-	-	-	-	Platisa et al., (2023)

[a] : Decay kinetics were calculated using a single-exponential function.

Table 3
Comparative performance of opsin-based GEVIs.

GEVI	Rhodopsin	Fluorophore	ΔF/F (%)	τ_{on} τ_1:τ_{on} fast (ms) τ_2:τ_{on} slow (ms) $\%_{\tau1}$: $\tau_1$component amplitude (%)			τ_{off} τ_1:τ_{off} fast (ms) τ_2:τ_{off} slow (ms) $\%_{\tau1}$: $\tau_1$component amplitude (%)			Reference
				τ_1 (ms)	τ_2 (ms)	$\%_{\tau1}$	τ_1 (ms)	τ_2 (ms)	$\%_{\tau1}$	
Microbial rhodopsin-based GEVIs										
Arch	Arch	Retinal	40	0.6	-	-	0.25	1.9	67	Kralj et al., (2011)
Archon1	Arch	Retinal	70	2.5	13	93	2.0	17	94	Piatkevich et al., (2018)
QuasAr6a	Arch	Retinal	73	2.6	21	96	2.1	31	98	Tian et al., (2023)
eFRET-based GEVI										
Ace2-mNeon	Ace2	mNeonGreen	-18	0.37	5.5	58	0.50	5.9	60	Gong et al., (2015)
Ace2-mNeon2	Ace2	mNeonGreen	-26	0.77	3.1	67	0.81	2.8	65	Kannan et al., (2022)
VARNAM	Ace2	mRuby3	-12	0.88	5.2	60	0.80	4.7	60	Kannan et al., (2018)
VARNAM2	Ace2	mRuby3	-19	0.50	1.9	68	0.48	3.1	72	Kannan et al., (2022)
Cepheid1b	Ace2	mScarlet	-32	-	-	-	-	-	-	Han et al., (2023)
$Voltron_{525}$	Ace2	JF525	-21	0.85	4.8	52	1.13	6.3	62	Abdelfattah et al., (2019)
$Voltron2_{525}$	Ace2	JF525	-34	0.67	3.3	78	0.89	4.7	45	Abdelfattah et al., (2023)
Positron	Ace2	JF525	18	0.63	19	85	0.64	37	90	Abdelfattah et al., (2020)
pAce	Ace2	mNeonGreen	31	0.51	1.5	82	0.61	3.2	78	Kannan et al., (2022)
pAceR	Ace2	mRuby3	28	2.4	5.4	54	1.9	7.2	58	Kannan et al., (2022)

Apart from fluorescent biosensors, imaging apparatuses are also crucial. Notably, rapid progress in microscopy for mesoscale imaging has facilitated the measurement of tens of thousands of neurons with single-cell resolution across a wide field of view (Ota et al., 2021; Sofroniew et al., 2016; Stirman et al., 2016). This mesoscale imaging is invaluable for exploring neural networks across an extensive range of brain regions. Mesoscale imaging is also applicable to fluorescent probes for intercellular signaling molecules and neuromodulators, in addition to neural activity, enabling the unraveling of complex intracellular processes that were previously outside of capabilities. Moreover, these techniques will provide profound insights into how multimodal sensory information is processed and integrated into the brain.

Despite these technological advancements, considerable challenges remain, particularly in managing and processing large-scale imaging data. For example, the mesoscopic two-photon microscopy (FASHIO2-PM) developed by Murayama and colleagues captures a 3 mm×3 mm field of view with 2048 × 2048 pixels at 7.5 Hz frame rate, yielding approximately 4 GB per minute, which is a substantial amount for functional imaging. (Ota et al., 2021). Similarly, voltage imaging, which requires higher frame rates to monitor millisecond-order membrane potential fluctuation, can produce approximately 8 GB per minute (512 × 128 pixels at 1 kHz) (Zhang et al., 2021). Furthermore, voltage imaging signals contain multiple waveforms, which require data processing for accurate definition of action potentials, subthreshold activities, and background noise. Such immense volume and complexity of the data demand a robust computational infrastructure and sophisticated, user-friendly analytical methods accessible to researchers in various fields. Furthermore, integrating various data types, including temporal and spatial data from both calcium imaging and voltage imaging, as well as genomics or proteomics, needs tools for advanced data integration and visualization (Csillag et al., 2023).

Another critical challenge is the standardization and sharing of big data in imaging. The lack of uniform formats for data storage and sharing hampers collaboration and constrains data reusability. Tackling this problem requires a collaborative approach from the scientific community to establish universal data standards and create platforms for open-access data sharing. These efforts would not only promote transparency and reproducibility in research but also encourage collaborative studies that can leverage the advantage of big data.

In conclusion, the integration of imaging technologies with big data analysis represents a significant advancement in the field of neuroscience. The ongoing development of sophisticated fluorescent biosensors and the improvement of data analysis algorithms are essential to deepen the understanding of mechanisms of higher brain functions. These concerted efforts are important to unravel complex physiological processes and contribute significantly to the development of novel therapeutic strategies for neurological and psychiatric disorders.

CRediT authorship contribution statement

Masayuki Sakamoto: Conceptualization, Visualization, Writing – original draft, Writing – review & editing. **Tatsushi Yokoyama:** Writing – review & editing.

Declaration of Competing Interest

The authors declare that the research was conducted in the absence of any commercial or financial relationships that could be construed as a potential conflict of interest.

Acknowledgments

This work was supported by AMED-PRIME (JP 23gm6510022 to M. S.), Interdisciplinary and Emerging Brain Research Program (iBrain/MINDS) (JP21wm0525004 to M.S.), ACT-X-JST (JPMJAX211K to T.Y.), JSPS KAKENHI (JP24H00861, JP23H02782 to M.S., JP21K15207 to T. Y.), Inamori Foundation (to M.S.), Mochida Memorial Foundation (to M. S.), KOSÉ Cosmetology Research Foundation (to M.S.).

References

Abdelfattah, A.S., Kawashima, T., Singh, A., Novak, O., Liu, H., Shuai, Y., Huang, Y.C., Campagnola, L., Seeman, S.C., Yu, J., Zheng, J., Grimm, J.B., Patel, R., Friedrich, J., Mensh, B.D., Paninski, L., Macklin, J.J., Murphy, G.J., Podgorski, K., Lin, B.J., Chen, T.W., Turner, G.C., Liu, Z., Koyama, M., Svoboda, K., Ahrens, M.B., Lavis, L.D., Schreiter, E.R., 2019. Bright and photostable chemigenetic indicators for extended in vivo voltage imaging. Science 365, 699–704.

Abdelfattah, A.S., Valenti, R., Zheng, J., Wong, A., Team, G.P., Podgorski, K., Koyama, M., Kim, D.S., Schreiter, E.R., 2020. A general approach to engineer positive-going eFRET voltage indicators. Nat. Commun. 11, 3444.

Abdelfattah, A.S., Zheng, J., Singh, A., Huang, Y.C., Reep, D., Tsegaye, G., Tsang, A., Arthur, B.J., Rehorova, M., Olson, C.V.L., Shuai, Y., Zhang, L., Fu, T.M., Milkie, D.E., Moya, M.V., Weber, T.D., Lemire, A.L., Baker, C.A., Falco, N., Zheng, Q., Grimm, J. B., Yip, M.C., Walpita, D., Chase, M., Campagnola, L., Murphy, G.J., Wong, A.M., Forest, C.R., Mertz, J., Economo, M.N., Turner, G.C., Koyama, M., Lin, B.J., Betzig, E., Novak, O., Lavis, L.D., Svoboda, K., Korff, W., Chen, T.W., Schreiter, E.R., Hasseman, J.P., Kolb, I., 2023. Sensitivity optimization of a rhodopsin-based fluorescent voltage indicator. Neuron 111, 1547–1563 e1549.

Akemann, W., Mutoh, H., Perron, A., Rossier, J., Knopfel, T., 2010. Imaging brain electric signals with genetically targeted voltage-sensitive fluorescent proteins. Nat. Methods 7, 643–649.

Bando, Y., Sakamoto, M., Kim, S., Ayzenshtat, I., Yuste, R., 2019. Comparative evaluation of genetically encoded voltage indicators. Cell Rep. 26, 802–813 e804.

Bando, Y., Wenzel, M., Yuste, R., 2021. Simultaneous two-photon imaging of action potentials and subthreshold inputs in vivo. Nat. Commun. 12, 7229.

Bayraktar, H., Fields, A.P., Kralj, J.M., Spudich, J.L., Rothschild, K.J., Cohen, A.E., 2012. Ultrasensitive measurements of microbial rhodopsin photocycles using photochromic FRET. Photochem. Photobiol. 88, 90–97.

Berridge, M.J., Lipp, P., Bootman, M.D., 2000. The versatility and universality of calcium signalling. Nat. Rev. Mol. Cell Biol. 1, 11–21.

Boyden, E.S., Zhang, F., Bamberg, E., Nagel, G., Deisseroth, K., 2005. Millisecond-timescale, genetically targeted optical control of neural activity. Nat. Neurosci. 8, 1263–1268.

Chen, T.W., Wardill, T.J., Sun, Y., Pulver, S.R., Renninger, S.L., Baohan, A., Schreiter, E. R., Kerr, R.A., Orger, M.B., Jayaraman, V., Looger, L.L., Svoboda, K., Kim, D.S., 2013. Ultrasensitive fluorescent proteins for imaging neuronal activity. Nature 499, 295–300.

Chow, B.Y., Han, X., Dobry, A.S., Qian, X., Chuong, A.S., Li, M., Henninger, M.A., Belfort, G.M., Lin, Y., Monahan, P.E., Boyden, E.S., 2010. High-performance genetically targetable optical neural silencing by light-driven proton pumps. Nature 463, 98–102.

Chu, M.W., Li, W.L., Komiyama, T., 2016. Balancing the robustness and efficiency of odor representations during learning. Neuron 92, 174–186.

Cornejo, V.H., Ofer, N., Yuste, R., 2022. Voltage compartmentalization in dendritic spines in vivo. Science 375, 82–86.

Csillag, V., Bizzozzero, M.H., Noble, J.C., Reinius, B., Fuzik, J., 2023. Voltage-Seq: all-optical postsynaptic connectome-guided single-cell transcriptomics. Nat. Methods 20, 1409–1416.

Dana, H., Mohar, B., Sun, Y., Narayan, S., Gordus, A., Hasseman, J.P., Tsegaye, G., Holt, G.T., Hu, A., Walpita, D., Patel, R., Macklin, J.J., Bargmann, C.I., Ahrens, M.B., Schreiter, E.R., Jayaraman, V., Looger, L.L., Svoboda, K., Kim, D.S., 2016. Sensitive red protein calcium indicators for imaging neural activity. Elife 5, e12727.

Dana, H., Sun, Y., Mohar, B., Hulse, B.K., Kerlin, A.M., Hasseman, J.P., Tsegaye, G., Tsang, A., Wong, A., Patel, R., Macklin, J.J., Chen, Y., Konnerth, A., Jayaraman, V., Looger, L.L., Schreiter, E.R., Svoboda, K., Kim, D.S., 2019. High-performance calcium sensors for imaging activity in neuronal populations and microcompartments. Nat. Methods 16, 649–657.

Deo, C., Abdelfattah, A.S., Bhargava, H.K., Berro, A.J., Falco, N., Farrants, H., Moeyaert, B., Chupanova, M., Lavis, L.D., Schreiter, E.R., 2021. The HaloTag as a general scaffold for far-red tunable chemigenetic indicators. Nat. Chem. Biol. 17, 718–723.

Duffet, L., Kosar, S., Panniello, M., Viberti, B., Bracey, E., Zych, A.D., Radoux-Mergault, A., Zhou, X., Dernic, J., Ravotto, L., Tsai, Y.C., Figueiredo, M., Tyagarajan, S.K., Weber, B., Stoeber, M., Gogolla, N., Schmidt, M.H., Adamantidis, A.R., Fellin, T., Burdakov, D., Patriarchi, T., 2022. A genetically encoded sensor for in vivo imaging of orexin neuropeptides. Nat. Methods 19, 231–241.

Ebina, T., Masamizu, Y., Tanaka, Y.R., Watakabe, A., Hirakawa, R., Hirayama, Y., Hira, R., Terada, S.I., Koketsu, D., Hikosaka, K., Mizukami, H., Nambu, A., Sasaki, E., Yamamori, T., Matsuzaki, M., 2018. Two-photon imaging of neuronal activity in motor cortex of marmosets during upper-limb movement tasks. Nat. Commun. 9, 1879.

Evans, S.W., Shi, D.Q., Chavarha, M., Plitt, M.H., Taxidis, J., Madruga, B., Fan, J.L., Hwang, F.J., van Keulen, S.C., Suomivuori, C.M., Pang, M.M., Su, S., Lee, S., Hao, Y. A., Zhang, G., Jiang, D., Pradhan, L., Roth, R.H., Liu, Y., Dorian, C.C., Reese, A.L., Negrean, A., Losonczy, A., Makinson, C.D., Wang, S., Clandinin, T.R., Dror, R.O., Ding, J.B., Ji, N., Golshani, P., Giocomo, L.M., Bi, G.Q., Lin, M.Z., 2023. A positively tuned voltage indicator for extended electrical recordings in the brain. Nat. Methods 20, 1104–1113.

Fenno, L.E., Ramakrishnan, C., Kim, Y.S., Evans, K.E., Lo, M., Vesuna, S., Inoue, M., Cheung, K.Y.M., Yuen, E., Pichamoorthy, N., Hong, A.S.O., Deisseroth, K., 2020. Comprehensive dual- and triple-feature intersectional single-vector delivery of diverse functional payloads to cells of behaving mammals. Neuron 107, 836–853 e811.

Gee, K.R., Brown, K.A., Chen, W.N., Bishop-Stewart, J., Gray, D., Johnson, I., 2000. Chemical and physiological characterization of fluo-4 Ca(2+)-indicator dyes. Cell Calcium 27, 97–106.

Gong, Y., Huang, C., Li, J.Z., Grewe, B.F., Zhang, Y., Eismann, S., Schnitzer, M.J., 2015. High-speed recording of neural spikes in awake mice and flies with a fluorescent voltage sensor. Science 350, 1361–1366.

Gong, Y., Wagner, M.J., Zhong Li, J., Schnitzer, M.J., 2014. Imaging neural spiking in brain tissue using FRET-opsin protein voltage sensors. Nat. Commun. 5, 3674.

Grienberger, C., Konnerth, A., 2012. Imaging calcium in neurons. Neuron 73, 862–885.

Grynkiewicz, G., Poenie, M., Tsien, R.Y., 1985. A new generation of Ca2+ indicators with greatly improved fluorescence properties. J. Biol. Chem. 260, 3440–3450.

Han, Y., Yang, J., Li, Y., Chen, Y., Ren, H., Ding, R., Qian, W., Ren, K., Xie, B., Deng, M., Xiao, Y., Chu, J., Zou, P., 2023. Bright and sensitive red voltage indicators for imaging action potentials in brain slices and pancreatic islets. Sci. Adv. 9, eadi4208.

Hashizume, R., Fujii, H., Mehta, S., Ota, K., Qian, Y., Zhu, W., Drobizhev, M., Nasu, Y., Zhang, J., Bito, H., Campbell, R.E., 2022. A genetically encoded far-red fluorescent calcium ion biosensor derived from a biliverdin-binding protein. Protein Sci. 31, e4440.

Ino, D., Tanaka, Y., Hibino, H., Nishiyama, M., 2022. A fluorescent sensor for real-time measurement of extracellular oxytocin dynamics in the brain. Nat. Methods 19, 1286–1294.

Inoue, M., Takeuchi, A., Horigane, S., Ohkura, M., Gengyo-Ando, K., Fujii, H., Kamijo, S., Takemoto-Kimura, S., Kano, M., Nakai, J., Kitamura, K., Bito, H., 2015. Rational design of a high-affinity, fast, red calcium indicator R-CaMP2. Nat. Methods 12, 64–70.

Inoue, M., Takeuchi, A., Manita, S., Horigane, S.I., Sakamoto, M., Kawakami, R., Yamaguchi, K., Otomo, K., Yokoyama, H., Kim, R., Yokoyama, T., Takemoto-Kimura, S., Abe, M., Okamura, M., Kondo, Y., Quirin, S., Ramakrishnan, C., Imamura, T., Sakimura, K., Nemoto, T., Kano, M., Fujii, H., Deisseroth, K., Kitamura, K., Bito, H., 2019. Rational Engineering of XCaMPs, a Multicolor GECI Suite for In Vivo Imaging of Complex Brain Circuit Dynamics. Cell 177, 1346–1360 e1324.

Jin, L., Han, Z., Platisa, J., Wooltorton, J.R., Cohen, L.B., Pieribone, V.A., 2012. Single action potentials and subthreshold electrical events imaged in neurons with a fluorescent protein voltage probe. Neuron 75, 779–785.

Kannan, M., Vasan, G., Haziza, S., Huang, C., Chrapkiewicz, R., Luo, J., Cardin, J.A., Schnitzer, M.J., Pieribone, V.A., 2022. Dual-polarity voltage imaging of the concurrent dynamics of multiple neuron types. Science 378, eabm8797.

Kannan, M., Vasan, G., Huang, C., Haziza, S., Li, J.Z., Inan, H., Schnitzer, M.J., Pieribone, V.A., 2018. Fast, in vivo voltage imaging using a red fluorescent indicator. Nat. Methods 15, 1108–1116.

Karigo, T., Kennedy, A., Yang, B., Liu, M., Tai, D., Wahle, I.A., Anderson, D.J., 2021. Distinct hypothalamic control of same- and opposite-sex mounting behaviour in mice. Nature 589, 258–263.

Kojima, K., Kurihara, R., Sakamoto, M., Takanashi, T., Kuramochi, H., Zhang, X.M., Bito, H., Tahara, T., Sudo, Y., 2020. Comparative studies of the fluorescence properties of microbial Rhodopsins: spontaneous emission versus photointermediate fluorescence. J. Phys. Chem. B 124, 7361–7367.

Kondo, M., Kobayashi, K., Ohkura, M., Nakai, J., Matsuzaki, M., 2017. Two-photon calcium imaging of the medial prefrontal cortex and hippocampus without cortical invasion. Elife 6, e26839.

Kondo, T., Saito, R., Otaka, M., Yoshino-Saito, K., Yamanaka, A., Yamamori, T., Watakabe, A., Mizukami, H., Schnitzer, M.J., Tanaka, K.F., Ushiba, J., Okano, H., 2018. Calcium transient dynamics of neural ensembles in the primary motor cortex of naturally behaving monkeys. Cell Rep. 24, 2191–2195 e2194.

Kralj, J.M., Douglass, A.D., Hochbaum, D.R., Maclaurin, D., Cohen, A.E., 2011. Optical recording of action potentials in mammalian neurons using a microbial rhodopsin. Nat. Methods 9, 90–95.

Kwon, T., Sakamoto, M., Peterka, D.S., Yuste, R., 2017. Attenuation of synaptic potentials in dendritic spines. Cell Rep. 20, 1100–1110.

Landhuis, E., 2017. Neuroscience: Big brain, big data. Nature 541, 559–561.

Li, J., Shang, Z., Chen, J.H., Gu, W., Yao, L., Yang, X., Sun, X., Wang, L., Wang, T., Liu, S., Li, J., Hou, T., Xing, D., Gill, D.L., Li, J., Wang, S.Q., Hou, L., Zhou, Y., Tang, A.H., Zhang, X., Wang, Y., 2023. Engineering of NEMO as calcium indicators with large dynamics and high sensitivity. Nat. Methods 20, 918–924.

Liu, Z., Lu, X., Villette, V., Gou, Y., Colbert, K.L., Lai, S., Guan, S., Land, M.A., Lee, J., Assefa, T., Zollinger, D.R., Korympidou, M.M., Vlasits, A.L., Pang, M.M., Su, S., Cai, C., Froudarakis, E., Zhou, N., Patel, S.S., Smith, C.L., Ayon, A., Bizouard, P., Bradley, J., Franke, K., Clandinin, T.R., Giovannucci, A., Tolias, A.S., Reimer, J., Dieudonne, S., St-Pierre, F., 2022. Sustained deep-tissue voltage recording using a fast indicator evolved for two-photon microscopy. Cell 185, 3408–3425 e3429.

Lu, X., Wang, Y., Liu, Z., Gou, Y., Jaeger, D., St-Pierre, F., 2023. Widefield imaging of rapid pan-cortical voltage dynamics with an indicator evolved for one-photon microscopy. Nat. Commun. 14, 6423.

Maclaurin, D., Venkatachalam, V., Lee, H., Cohen, A.E., 2013. Mechanism of voltage-sensitive fluorescence in a microbial rhodopsin. Proc. Natl. Acad. Sci. USA 110, 5939–5944.
Marshall, J.D., Li, J.Z., Zhang, Y., Gong, Y., St-Pierre, F., Lin, M.Z., Schnitzer, M.J., 2016. Cell-type-specific optical recording of membrane voltage dynamics in freely moving Mice. Cell 167, 1650–1662 e1615.
Michikawa, T., Yoshida, T., Kuroki, S., Ishikawa, T., Kakei, S., Kimizuka, R., Saito, A., Yokota, H., Shimizu, A., Itohara, S., Miyawaki, A., 2021. Distributed sensory coding by cerebellar complex spikes in units of cortical segments. Cell Rep. 37, 109966.
Miyawaki, A., Llopis, J., Heim, R., McCaffery, J.M., Adams, J.A., Ikura, M., Tsien, R.Y., 1997. Fluorescent indicators for Ca2+ based on green fluorescent proteins and calmodulin. Nature 388, 882–887.
Mohr, M.A., Bushey, D., Aggarwal, A., Marvin, J.S., Kim, J.J., Marquez, E.J., Liang, Y., Patel, R., Macklin, J.J., Lee, C.Y., Tsang, A., Tsegaye, G., Ahrens, A.M., Chen, J.L., Kim, D.S., Wong, A.M., Looger, L.L., Schreiter, E.R., Podgorski, K., 2020. jYCaMP: an optimized calcium indicator for two-photon imaging at fiber laser wavelengths. Nat. Methods 17, 694–697.
Murata, Y., Iwasaki, H., Sasaki, M., Inaba, K., Okamura, Y., 2005. Phosphoinositide phosphatase activity coupled to an intrinsic voltage sensor. Nature 435, 1239–1243.
Nagai, T., Yamada, S., Tominaga, T., Ichikawa, M., Miyawaki, A., 2004. Expanded dynamic range of fluorescent indicators for Ca(2+) by circularly permuted yellow fluorescent proteins. Proc. Natl. Acad. Sci. USA 101, 10554–10559.
Nakai, J., Ohkura, M., Imoto, K., 2001. A high signal-to-noise Ca(2+) probe composed of a single green fluorescent protein. Nat. Biotechnol. 19, 137–141.
Neher, E., 1998. Usefulness and limitations of linear approximations to the understanding of Ca++ signals. Cell Calcium 24, 345–357.
Neher, E., Sakmann, B., 1976. Single-channel currents recorded from membrane of denervated frog muscle fibres. Nature 260, 799–802.
Ohkura, M., Sasaki, T., Kobayashi, C., Ikegaya, Y., Nakai, J., 2012. An improved genetically encoded red fluorescent Ca2+ indicator for detecting optically evoked action potentials. PLoS One 7, e39933.
Ota, K., Oisi, Y., Suzuki, T., Ikeda, M., Ito, Y., Ito, T., Uwamori, H., Kobayashi, K., Kobayashi, M., Odagawa, M., Matsubara, C., Kuroiwa, Y., Horikoshi, M., Matsushita, J., Hioki, H., Ohkura, M., Nakai, J., Oizumi, M., Miyawaki, A., Aonishi, T., Ode, T., Murayama, M., 2021. Fast, cell-resolution, contiguous-wide two-photon imaging to reveal functional network architectures across multi-modal cortical areas. Neuron 109, 1810–1824 e1819.
Peterka, D.S., Takahashi, H., Yuste, R., 2011. Imaging voltage in neurons. Neuron 69, 9–21.
Piatkevich, K.D., Bensussen, S., Tseng, H.A., Shroff, S.N., Lopez-Huerta, V.G., Park, D., Jung, E.E., Shemesh, O.A., Straub, C., Gritton, H.J., Romano, M.F., Costa, E., Sabatini, B.L., Fu, Z., Boyden, E.S., Han, X., 2019. Population imaging of neural activity in awake behaving mice. Nature 574, 413–417.
Piatkevich, K.D., Jung, E.E., Straub, C., Linghu, C., Park, D., Suk, H.J., Hochbaum, D.R., Goodwin, D., Pnevmatikakis, E., Pak, N., Kawashima, T., Yang, C.T., Rhoades, J.L., Shemesh, O., Asano, S., Yoon, Y.G., Freifeld, L., Saulnier, J.L., Riegler, C., Engert, F., Hughes, T., Drobizhev, M., Szabo, B., Ahrens, M.B., Flavell, S.W., Sabatini, B.L., Boyden, E.S., 2018. A robotic multidimensional directed evolution approach applied to fluorescent voltage reporters. Nat. Chem. Biol. 14, 352–360.
Platisa, J., Ye, X., Ahrens, A.M., Liu, C., Chen, I.A., Davison, I.G., Tian, L., Pieribone, V. A., Chen, J.L., 2023. High-speed low-light in vivo two-photon voltage imaging of large neuronal populations. Nat. Methods 20, 1095–1103.
Qian, Y., Piatkevich, K.D., Mc Larney, B., Abdelfattah, A.S., Mehta, S., Murdock, M.H., Gottschalk, S., Molina, R.S., Zhang, W., Chen, Y., Wu, J., Drobizhev, M., Hughes, T. E., Zhang, J., Schreiter, E.R., Shoham, S., Razansky, D., Boyden, E.S., Campbell, R.E., 2019. A genetically encoded near-infrared fluorescent calcium ion indicator. Nat. Methods 16, 171–174.
Sakamoto, M., Inoue, M., Takeuchi, A., Kobari, S., Yokoyama, T., Horigane, S.-i, Takemoto-Kimura, S., Abe, M., Sakimura, K., Kano, M., Kitamura, K., Fujii, H., Bito, H., 2022. A Flp-dependent G-CaMP9a transgenic mouse for neuronal imaging in vivo. Cell Rep. Methods 2, 100168.
Schneider, S., Lee, J.H., Mathis, M.W., 2023. Learnable latent embeddings for joint behavioural and neural analysis. Nature 617, 360–368.
Siegel, M.S., Isacoff, E.Y., 1997. A genetically encoded optical probe of membrane voltage. Neuron 19, 735–741.
Smetters, D., Majewska, A., Yuste, R., 1999. Detecting action potentials in neuronal populations with calcium imaging. Methods 18, 215–221.
Sofroniew, N.J., Flickinger, D., King, J., Svoboda, K., 2016. A large field of view two-photon mesoscope with subcellular resolution for in vivo imaging. Elife 5, e14472.
Stirman, J.N., Smith, I.T., Kudenov, M.W., Smith, S.L., 2016. Wide field-of-view, multi-region, two-photon imaging of neuronal activity in the mammalian brain. Nat. Biotechnol. 34, 857–862.
Storace, D., Sepehri Rad, M., Kang, B., Cohen, L.B., Hughes, T., Baker, B.J., 2016. Toward better genetically encoded sensors of membrane potential. Trends Neurosci. 39, 277–289.
Thestrup, T., Litzlbauer, J., Bartholomaus, I., Mues, M., Russo, L., Dana, H., Kovalchuk, Y., Liang, Y., Kalamakis, G., Laukat, Y., Becker, S., Witte, G., Geiger, A., Allen, T., Rome, L.C., Chen, T.W., Kim, D.S., Garaschuk, O., Griesinger, C., Griesbeck, O., 2014. Optimized ratiometric calcium sensors for functional in vivo imaging of neurons and T lymphocytes. Nat. Methods 11, 175–182.
Tian, H., Davis, H.C., Wong-Campos, J.D., Park, P., Fan, L.Z., Gmeiner, B., Begum, S., Werley, C.A., Borja, G.B., Upadhyay, H., Shah, H., Jacques, J., Qi, Y., Parot, V., Deisseroth, K., Cohen, A.E., 2023. Video-based pooled screening yields improved far-red genetically encoded voltage indicators. Nat. Methods 20, 1082–1094.
Tsien, R.Y., Pozzan, T., Rink, T.J., 1982. Calcium homeostasis in intact lymphocytes: cytoplasmic free calcium monitored with a new, intracellularly trapped fluorescent indicator. J. Cell Biol. 94, 325–334.
Tsutsui, H., Karasawa, S., Okamura, Y., Miyawaki, A., 2008. Improving membrane voltage measurements using FRET with new fluorescent proteins. Nat. Methods 5, 683–685.
Unger, E.K., Keller, J.P., Altermatt, M., Liang, R., Matsui, A., Dong, C., Hon, O.J., Yao, Z., Sun, J., Banala, S., Flanigan, M.E., Jaffe, D.A., Hartanto, S., Carlen, J., Mizuno, G.O., Borden, P.M., Shivange, A.V., Cameron, L.P., Sinning, S., Underhill, S.M., Olson, D. E., Amara, S.G., Temple Lang, D., Rudnick, G., Marvin, J.S., Lavis, L.D., Lester, H.A., Alvarez, V.A., Fisher, A.J., Prescher, J.A., Kash, T.L., Yarov-Yarovoy, V., Gradinaru, V., Looger, L.L., Tian, L., 2020. Directed evolution of a selective and sensitive serotonin sensor via machine learning. Cell 183, 1986–2002 e1926.
Villette, V., Chavarha, M., Dimov, I.K., Bradley, J., Pradhan, L., Mathieu, B., Evans, S.W., Chamberland, S., Shi, D., Yang, R., Kim, B.B., Ayon, A., Jalil, A., St-Pierre, F., Schnitzer, M.J., Bi, G., Toth, K., Ding, J., Dieudonne, S., Lin, M.Z., 2019. Ultrafast two-photon imaging of a high-gain voltage indicator in awake behaving mice. Cell 179, 1590–1608 e1523.
Wei, Z., Lin, B.J., Chen, T.W., Daie, K., Svoboda, K., Druckmann, S., 2020. A comparison of neuronal population dynamics measured with calcium imaging and electrophysiology. PLoS Comput. Biol. 16, e1008198.
Yokoyama, T., Manita, S., Uwamori, H., Tajiri, M., Imayoshi, I., Yagishita, S., Murayama, M., Kitamura, K., Sakamoto, M., 2024. A multicolor suite for deciphering population coding of calcium and cAMP in vivo. Nat. Methods 21, 897–907.
Yukinaga, H., Hagihara, M., Tsujimoto, K., Chiang, H.L., Kato, S., Kobayashi, K., Miyamichi, K., 2022. Recording and manipulation of the maternal oxytocin neural activities in mice. Curr. Biol. 32, 3821–3829 e3826.
Yuste, R., Bargmann, C., 2017. Toward a global BRAIN initiative. Cell 168, 956–959.
Zhang, Y., Rozsa, M., Liang, Y., Bushey, D., Wei, Z., Zheng, J., Reep, D., Broussard, G.J., Tsang, A., Tsegaye, G., Narayan, S., Obara, C.J., Lim, J.X., Patel, R., Zhang, R., Ahrens, M.B., Turner, G.C., Wang, S.S., Korff, W.L., Schreiter, E.R., Svoboda, K., Hasseman, J.P., Kolb, I., Looger, L.L., 2023. Fast and sensitive GCaMP calcium indicators for imaging neural populations. Nature 615, 884–891.
Zhang, X.M., Yokoyama, T., Sakamoto, M., 2021. Imaging voltage with microbial Rhodopsins. Front. Mol. Biosci. 8, 738829.
Zhao, Y., Araki, S., Wu, J., Teramoto, T., Chang, Y.F., Nakano, M., Abdelfattah, A.S., Fujiwara, M., Ishihara, T., Nagai, T., Campbell, R.E., 2011. An expanded palette of genetically encoded Ca(2)(+) indicators. Science 333, 1888–1891.
Zhuo, Y., Luo, B., Yi, X., Dong, H., Miao, X., Wan, J., Williams, J.T., Campbell, M.G., Cai, R., Qian, T., Li, F., Weber, S.J., Wang, L., Li, B., Wei, Y., Li, G., Wang, H., Zheng, Y., Zhao, Y., Wolf, M.E., Zhu, Y., Watabe-Uchida, M., Li, Y., 2023. Improved green and red GRAB sensors for monitoring dopaminergic activity in vivo. Nat. Methods 21, 680–691.
Zou, P., Zhao, Y., Douglass, A.D., Hochbaum, D.R., Brinks, D., Werley, C.A., Harrison, D. J., Campbell, R.E., Cohen, A.E., 2014. Bright and fast multicoloured voltage reporters via electrochromic FRET. Nat. Commun. 5, 4625.